applied sciences

MDPI

Article

Global Dynamics and Implications of an HBV Model with Proliferating Infected Hepatocytes

Sarah Hews [1], Steffen Eikenberry [2], John D. Nagy [2,3], Tin Phan [2] and Yang Kuang [2,*]

[1] School of Natural Science, Hampshire College, Amherst, MA 01002, USA; sarahhews@gmail.com
[2] School of Mathematical and Statistical Sciences, Arizona State University, Tempe, AZ 85281, USA; seikenbe@asu.edu (S.E.); John.Nagy@asu.edu (J.D.N.); ttphan4@asu.edu (T.P.)
[3] Department of Life Sciences, Scottsdale Community College, Scottsdale, AZ 85256, USA
* Correspondence: Kuang@asu.edu

Abstract: Chronic hepatitis B (HBV) infection is a major cause of human suffering, and a number of mathematical models have examined the within-host dynamics of the disease. Most previous models assumed that infected hepatocytes do not proliferate; however, the effect of HBV infection on hepatocyte proliferation is controversial, with conflicting data showing both induction and inhibition of proliferation. With a family of ordinary differential equation (ODE) models, we explored the dynamical impact of proliferation among HBV-infected hepatocytes. Here, we show that infected hepatocyte proliferation in this class of models generates a threshold that divides the dynamics into two categories. Sufficiently compromised proliferation in infected cells produces complex dynamics characterized by oscillating viral loads, whereas higher proliferation generates straightforward dynamics that always results in chronic infection, sometimes with liver failure. A global stability result of the liver failure state was included as it is unique to this class of models. Finally, the model analysis motivated a testable biological hypothesis: Healthy hepatocytes are present in chronic HBV infection if and only if the proliferation of infected hepatocytes is severely impaired.

Keywords: HBV; ratio-dependent transformation; logistic hepatocyte growth; origin stability; Hopf bifurcation

Citation: Hews, S.; Eikenberry, S.; Nagy, J.D.; Phan, T.; Kuang, Y. Global Dynamics and Implications of an HBV Model with Proliferating Infected Hepatocytes. *Appl. Sci.* **2021**, *11*, 8176. https://doi.org/10.3390/app11178176

Academic Editor: Fabio La Foresta

Received: 8 July 2021
Accepted: 1 September 2021
Published: 3 September 2021

1. Introduction

Hepatitis B virus (HBV) is a global public health problem. It infects hepatocytes, the main cells found in the liver, and can lead to chronic liver disease, cirrhosis, and liver cancer. As of 2015, over 250 million people worldwide are chronically infected with HBV, with the majority of these cases in Asia, Sub-Saharan Africa, parts of the Arabian Peninsula, the South Pacific, tropical South America, and arctic North America, with Asia unique in the degree of hepatitis burden. In areas where HBV is highly endemic, the infection is spread primarily neonatally from infected mothers to their children, with as many as 90% of infants exposed to the virus developing chronic infections. Young children also remain susceptible to chronic infection, while fewer than 5% of exposed adults, who are otherwise healthy, will go on to develop chronic disease. Besides vertical transmission, HBV may be contracted through any blood-borne exposure, including sexual contact, needle sharing, or blood transfusion [1,2]. Although the global burden of viral hepatitis is in decline—in large part due to a nearly 100% effective vaccine, near universal screening of blood products, and more effective treatments—the vaccine is still not implemented widely enough, and a significant number of cases persist even in developed countries [3]. Treatment for chronic HBV can reduce the risk of developing cirrhosis and liver cancer, but generally does not result in a cure and often must be taken lifelong once initiated [2].

Despite these recent clinical advances and the disease's global significance, its pathogenesis remains poorly understood. A widely accepted hypothesis suggests that HBV is not directly cytopathic; rather, liver inflammation and subsequent complications caused

by HBV are generated by immune attack on infected cells [4–6]. Considerable evidence supports this hypothesis [4,5,7,8], However, the extent and nature of the virus's cytopathicity remain unresolved [9]. In particular, very little is known about how viral infection affects proliferation. In the experimental literature, the effect of HBV infection on hepatocyte proliferation is controversial, with conflicting data showing both induction and inhibition of proliferation [10]. In addition, infection has been correlated with both pro- and anti-apoptotic effects on hepatocytes [11]. HBV X protein has severely impaired liver regeneration in some mouse models [11–13], but had little effect in others [14]. It is possible that natural variation in the HBV virus itself may explain these conflicting results [10]. Here, we study the dynamical implications of the proliferation of infected hepatocytes.

Mathematical models have been applied to a wide variety of viral illnesses, and HBV is no exception, with scores of modeling works published in recent years (see, e.g., recent reviews by Goyal et al. [15] and Ciupe [16]). Previous models have mainly, though not exclusively, focused on chronic infections and were originally adapted from HIV models, including at least three state variables: healthy hepatocytes, x, infected hepatocytes, y, and free virions, v. The basic virus infection model (BVIM), presented by Nowak et al. [17,18], assumes that healthy hepatocytes are produced by some constant influx term, λ, healthy hepatocytes die at per-capita rate d, infected hepatocytes die at per-capita rate a, and infection occurs according to *mass action kinetics*, with coefficient β. Infectious virions are produced by infected hepatocytes at rate γ and die at rate μ, giving the model:

$$\frac{dx}{dt} = \lambda - dx - \beta xv, \tag{1}$$

$$\frac{dy}{dt} = \beta xv - ay, \tag{2}$$

$$\frac{dv}{dt} = \gamma y - \mu v. \tag{3}$$

In this model, the immune response to infection is represented by an elevated death rate in infected hepatocytes, $a > d$, and by the destruction of free virions at rate μ. Such simple linear dynamics are clearly inappropriate for modeling the adaptive immune system's response to acute infection, but may be a reasonable first approximation in the case of established, chronic infection. Extensions and variations of the BVIM model have been introduced to study the rich dynamics of HIV infection and treatment [19,20]. This basic framework has been extended and modified to study different aspects of HBV infection. Multiple works have modeled the immune response in at least some detail [16,21–24] and considered the interplay between the immune response and imposed treatments [25,26]. Drug treatment, with or without the immune response, can also be incorporated into this basic framework—e.g., [27–29]. Some drugs interfere with virion production, which can be simply modeled as a decreased virion production rate when treatment is on, while others decrease the magnitude of the infection term [28].

While different biological behaviors can be added in different ways, special care to the basic model construction and its implicit assumptions is warranted. Restricting our attention to chronic infection and ignoring any adaptive or evolving immune response, the BVIM still makes at least three basic assumptions incompatible with biology that have major effects on the model dynamics:

1. Infection is a mass action process;
2. Healthy hepatocytes are produced by a constant influx;
3. Infected hepatocytes do not reproduce.

As shown by Gourley et al. [30], the assumption of mass action kinetics for infection yields a basic reproductive number that is dependent on the homeostatic liver size, λ/d, and thus results in the biologically implausible prediction that an individual's susceptibility to infection depends on liver mass. Replacing the mass action term with a standard incidence term, as in [30,31], eliminates this dependence. The standard incidence term in generic viral infection models also received theoretical treatment in [32,33]. Furthermore, the concept

of mass action kinetics is borrowed from chemical kinetics, where reaction rates increase in proportion to the concentration of all involved reactants [34]. As a solid organ with a highly stereotyped cellular architecture, the actual density of hepatocytes is not expected to vary appreciably between individuals or disease states, further arguing against the mass action formulation and for a standard incidence (or other) term better suited to the physical system.

The injured liver is clearly not replenished by a constant influx of cells. Rather, liver regeneration is driven by widespread hepatocyte proliferation in a process that is modeled very well, at least heuristically, by logistic growth (see Eikenberry et al. [35] for a detailed justification of the logistic growth term). As shown in [35,36], replacing the constant influx of healthy hepatocytes with logistic growth that depends on the total liver mass (both healthy and infected hepatocytes) greatly affects the model dynamics.

The analysis of Hews et al. [36] also derived two new indices, the cellular vitality index, R^*, and the liver failure index, R_f, that, in addition to the well-known basic reproductive number, R_0, partition the parameter space into distinct dynamical regions. This model admits three potential steady states, corresponding to complete obliteration of the liver ($x = y = v = 0$), chronic liver infection ($x, y, v > 0$), and absence of disease ($x > 0$; $y, v = 0$). Interestingly, there exists a region of the parameter space where all of the states are unstable. In this region, hepatocyte populations (both healthy and infected) and viral loads exhibit sustained oscillation. Furthermore, for each of these three steady states, there exist parameter regimes in which the steady state is asymptotically stable. Ciupe et al. [22,37] also considered logistic growth for hepatocytes in the more complex setting of acute infection, and logistic growth has been considered in other works as well [38,39]; however, the precise dynamical effect of this term in these models is unclear.

While the effects of modifying the first two assumptions to more biologically realistic alternatives have been thoroughly studied [30,31,35,36], here we make a special study of the dynamic implications of relaxing the assumption that infected hepatocytes do not reproduce. It must be noted that many HBV infection models also remove this assumption [16,38–43], with Dahari et al. [38], for example, suggesting that differing proliferation dynamics among healthy and infected hepatocytes could help explain varying patterns of viral load decays observed after treatment initiation, while Reluga et al. [39] applied a similar model to chronic hepatitis C viral dynamics. Goyal et al. [42] suggested that infected hepatocytes proliferating to produce uninfected daughter cells may be an important dynamic in preventing acute HBV infection, which directly affects up to 99% of hepatocytes, from progressing to the chronic state. Ciupe and colleagues [22,44] also considered the possibility that infected cells may recover from infection via a noncytolytic mechanism and thereafter become refractory to further infection (essentially a within-host "susceptible–infected–recovered" framework), with logistic growth dynamics for all hepatocyte classes, but mass action infection dynamics. Indeed, mass action infection kinetics remain common across those HBV models that do employ logistic growth (although, see, e.g., [26] for an exception), and the precise dynamical implications of logistic growth in both infected and uninfected hepatocytes are rarely studied. Furthermore, given the lack of consensus on the infection's effect on proliferation, as a first approximation, we assumed that infected hepatocytes proliferate no faster than healthy hepatocytes.

We rigorously explored how adding proliferation in infected hepatocytes, in addition to logistic growth in general and the standard incidence term for viral infection, affects the dynamics of basic chronic HBV models. The analysis of these models is not intended to provide evidence as to whether infected hepatocytes proliferate or not, but does yield a testable biological hypothesis: healthy hepatocytes are present in chronic HBV infection if and only if the proliferation of infected hepatocytes is severely impaired. The following section justifies this hypothesis.

2. Model Development and Dynamics

We assumed that infected hepatocytes proliferate at a rate less than or equal to the rate of proliferation of healthy hepatocytes. As many other chronic HBV models, we omitted a complex immune response. Therefore, our model has a population of healthy hepatocytes, $x(t)$, a population of infected hepatocytes, $y(t)$, and a population of free virions, $v(t)$,

$$\frac{dx}{dt} = rx(t)\left(1 - \frac{x(t)+y(t)}{K}\right) - \frac{\beta v(t)x(t)}{x(t)+y(t)}, \tag{4}$$

$$\frac{dy}{dt} = \rho y(t)\left(1 - \frac{(x(t)+y(t)}{K}\right) + \frac{\beta v(t)x(t)}{x(t)+y(t)} - ay(t), \tag{5}$$

$$\frac{dv}{dt} = \gamma y(t) - \mu v(t). \tag{6}$$

A logistic growth term is also used for the proliferation of healthy and infected hepatocytes with r and ρ as the maximum proliferation rates and K as the carrying capacity. The infection rate is β; the death rate of infected hepatocytes is a; the number of free virions produced per infected hepatocyte is γ; the death rate of virions is μ.

The basic reproduction number, R_0, is the same as with all previous models that assume a standard incidence term for infection,

$$R_0 = \frac{\beta\gamma}{a\mu}.$$

The cellular vitality index, R^*, first introduced in Hews et al. [36], incorporates the rates of healthy hepatocyte proliferation, infected hepatocyte proliferation, and infected hepatocyte lifespan, and it roughly represents the capacity of the healthy liver to regenerate. For the model (4)–(6),

$$R^* = \frac{r-\rho+a}{a}.$$

For clarification, R_0 has the standard definition, which is the expected number of secondary infections per primary infection in a completely susceptible population. On the other hand, R^* is the point when E^*, the chronic infection state with a nonzero healthy hepatocyte population, ceases to exist given that $R_0 > 1$. Since R^* depends on the proliferation and death rates of hepatocytes and relates to the possible collapse of the system (to the extinction equilibrium), R^* can be thought of as representing the capacity of the healthy liver to regenerate. From this, it can be seen that increasing either the proliferation or lifespan of infected hepatocytes impairs the ability of the infected liver to regenerate, while greater proliferation in healthy hepatocytes is beneficial.

In the following subsections, we present two different proliferation scenarios that differ in the maximum proliferation rate of infected hepatocytes. In the first of these, we assumed that infected hepatocytes proliferate at the same rate as healthy hepatocytes. In the second, we assumed that hepatocytes proliferate at a non-negligible rate that is nevertheless lower than that of healthy hepatocytes. We assumed nonnegative initial conditions for both models. One can use the methods of Hews et al. [36] to show rigorously that solutions in both models remain bounded and nonnegative.

2.1. Infected Hepatocytes Proliferating at the Same Rate

We assumed that healthy and infected hepatocytes proliferate at the same rate and therefore set $\rho = r$ and arrive at the first model:

$$\frac{dx}{dt} = rx(t)\left(1 - \frac{x(t)+y(t)}{K}\right) - \frac{\beta v(t)x(t)}{x(t)+y(t)}, \tag{7}$$

$$\frac{dy}{dt} = ry(t)\left(1 - \frac{(x(t)+y(t)}{K}\right) + \frac{\beta v(t)x(t)}{x(t)+y(t)} - ay(t), \tag{8}$$

$$\frac{dv}{dt} = \gamma y(t) - \mu v(t). \tag{9}$$

As mentioned above, the basic reproduction number is:

$$R_0 = \frac{\beta\gamma}{a\mu},$$

and the cellular vitality index is:

$$R^* = \frac{r - r + a}{a} = 1.$$

If $R_0 \neq 1$, there are three steady states of (7)–(9):

$$E_0 = (0,0,0), \qquad E_f = (K,0,0), \qquad E_i = \left(0, \frac{K(r-a)}{r}, \frac{\gamma K(r-a)}{r\mu}\right).$$

If $R_0 = 1$, there are infinitely many positive steady states. Hence, in the following, we assumed that $R_0 \neq 1$. Let E_0, E_f, and E_i be the liver failure, disease-free, and infected states, respectively. The liver failure state exists since,

$$\lim_{(x,y,v)\to(0,0,0)} \frac{\beta v x}{x+y} = 0.$$

Notice that the infected state E_i does not allow a population of healthy hepatocytes. Therefore, chronic infection in this model is always characterized by complete infection of the liver. It should be pointed out that models using a mass action term instead of the standard incidence for infection do admit chronic infections that maintain a healthy cell population, but we rejected these models for reasons already specified [30].

Notice that E_i only exists in the positive cone and is therefore biologically relevant only when $r > a$. At E_i, the total number of hepatocytes is $\frac{K(r-a)}{r}$; therefore, increasing proliferation (r) or decreasing mortality (a) rates increases equilibrium liver mass (assumed to be proportional to the number of hepatocytes). If the proliferation rate is greater than the death rate of infected hepatocytes then whether the infection becomes chronic depends on the reproduction rate. If $R_0 < 1$, the liver is free of infection, and if $R_0 > R^* = 1$, the liver becomes completely infected and the hepatocyte population is reduced compared to the healthy liver.

Proposition 1. *Given the system (7)–(9), if $r > a$, then E_i exists and the following results hold.*
a. If $R_0 < 1$, then E_f is locally asymptotically stable and E_i is a saddle point;
b. If $R_0 > 1$, then E_f is unstable and E_i is locally asymptotically stable.

The proofs are omitted as they involve straightforward linearization techniques. Since E_i always exists when $r > a$ and is a saddle when $R_0 < 1$, global stability for E_f cannot be determined. Figure 1 shows a bifurcation diagram of a with $r > a$. Healthy hepatocytes and infected hepatocytes are plotted separately so it is clear that the number of infected hepatocytes and virions is an increasing function of a.

If $r < a$, then the only steady states are E_0 and E_f. As with traditional viral infection models, E_f is globally stable when $R_0 < 1$.

Theorem 2. *If $r < a$ and $R_0 < 1$, E_f is globally stable.*

Proof. Let $(y(t), v(t))$ be a solution of:

$$\frac{dy(t)}{dt} \leq ry(t) + \beta v(t) - ay(t), \tag{10}$$

$$\frac{dv(t)}{dt} \leq \gamma y(t) - \mu v(t). \tag{11}$$

Let $(Y(t), V(t))$ be a solution of:

$$\frac{dY(t)}{dt} = \beta V(t) - (a - r)Y(t), \tag{12}$$

$$\frac{dV(t)}{dt} = \gamma Y(t) - \mu V(t). \tag{13}$$

$(Y, V) = (0, 0)$ is the only steady state of (12) and (13) and is locally asymptotically stable when $r < a$ and $R_0 < 1$. Since (12) and (13) is a cooperative system, and therefore monotone, all solutions of (12) and (13) will approach $(0, 0)$.

Let $y_0 = Y_0$, $v_0 = V_0$; then by the comparison theorem, $(y(t), v(t)) \leq (Y(t), V(t))$ for $t > 0$. Therefore,

$$0 \leq \liminf_{t\to\infty} y(t) \leq \limsup_{t\to\infty} y(t) \leq \lim_{t\to\infty} Y(t) = 0,$$

$$0 \leq \liminf_{t\to\infty} v(t) \leq \limsup_{t\to\infty} v(t) \leq \lim_{t\to\infty} V(t) = 0.$$

Therefore, by the squeeze theorem,

$$\liminf_{t\to\infty} y(t) = \limsup_{t\to\infty} y(t) = 0,$$

$$\liminf_{t\to\infty} v(t) = \limsup_{t\to\infty} v(t) = 0.$$

□

Since E_0 and E_f are the only two steady states, there can neither be a chronic stable state nor sustained oscillations.

Biologically, as long as hepatocytes proliferate faster than the infected hepatocytes die, the liver will survive. Since the number of infected hepatocytes at E_i is $\frac{K(r-a)}{r}$, the greater the hepatocyte proliferation rate and the smaller the death rate of infected hepatocytes, the greater the equilibrium number of hepatocytes in the liver. This result is intuitively clear.

According to Proposition 1(b), this model presents the following biological hypothesis: if healthy and infected hepatocytes proliferate at the same rate, then there will not be a significant population of healthy cells in the liver during chronic infection. Furthermore, patients would be unlikely to experience oscillations in viral load and liver mass, dynamics that are present in models without infected hepatocyte proliferation.

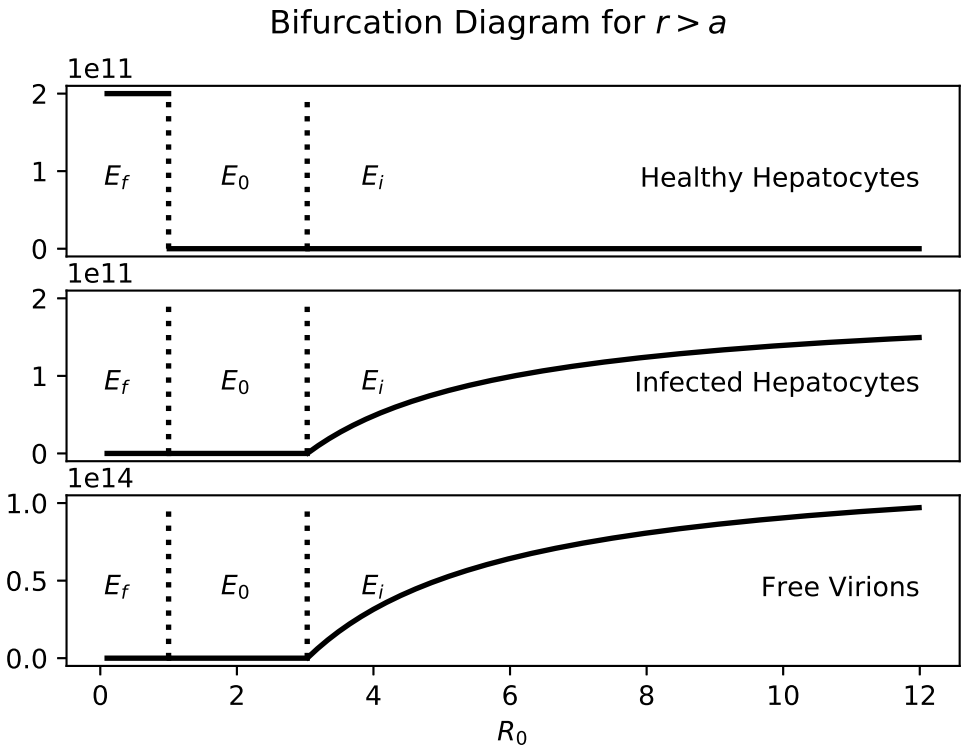

Figure 1. Bifurcation diagram showing, from top to bottom, equilibrium healthy hepatocyte, infected hepatocyte, and free virion populations as a function of R_0, where R_0 is varied via a. Other parameter values are fixed at: $r = 0.3$, $\mu = 0.693$, $\beta = 0.0014$, $\gamma = 450$, $K = 2 \times 10^{11}$.

2.2. Infected Hepatocytes Proliferating at a Different Rate

Since the data are inconclusive as to the proliferation rate of infected hepatocytes, we next explored the dynamical implication of infected hepatocytes proliferating at a smaller rate than healthy hepatocytes. The only change made to (7)–(9) is that the maximum proliferation rate for the infected hepatocytes is changed from r to ρ,

$$\frac{dx}{dt} = rx(t)\left(1 - \frac{x(t)+y(t)}{K}\right) - \frac{\beta v(t)x(t)}{x(t)+y(t)}, \tag{14}$$

$$\frac{dy}{dt} = \rho y(t)\left(1 - \frac{(x(t)+y(t)}{K}\right) + \frac{\beta v(t)x(t)}{x(t)+y(t)} - ay(t), \tag{15}$$

$$\frac{dv}{dt} = \gamma y(t) - \mu v(t), \tag{16}$$

where $\rho < r$. The basic reproduction number, R_0, is again,

$$R_0 = \frac{\beta\gamma}{a\mu}.$$

The cellular vitality index, R^*, is slightly modified to account for the proliferation of infected hepatocytes. In particular,

$$R^* = \frac{a + r - \rho}{a}.$$

In addition to the three equilibria admitted by the model (7)–(9), the system (14)–(16) allows an additional steady state representing chronic infection, seen in Hews et al. [36].

The entire set of equilibria therefore can include the following: $E_0 = (0,0,0)$, $E_f = (K,0,0)$, $E_i = \left(0, \frac{K(\rho-a)}{\rho}, \frac{\gamma K(\rho-a)}{\rho\mu}\right)$, and $E^* = (x^*, y^*, v^*)$, where:

$$\begin{aligned} x^* &= \frac{Kra}{(r-\rho)^2}\left(1-\frac{\rho}{r}R_0\right)\left(\frac{R^*}{R_0}-1\right), \\ y^* &= \frac{Kra}{(r-\rho)^2}(R_0-1)\left(\frac{R^*}{R_0}-1\right), \\ v^* &= \frac{K\gamma ra}{\mu(r-\rho)^2}(R_0-1)\left(\frac{R^*}{R_0}-1\right). \end{aligned}$$

Notice that E_i only exists if $\rho > a$ and E^* only exists if $1 < R_0 < R^*$ and the maximum proliferation rate of infected hepatocytes is sufficiently small, namely:

$$R_0 < \frac{r}{\rho}.$$

Figure 2 highlights the relationship between R_0 and ρ. As R_0 increases into the biologically relevant range of 6–8, The maximum value of ρ that admits a chronic steady state is quite small, less than 0.1.

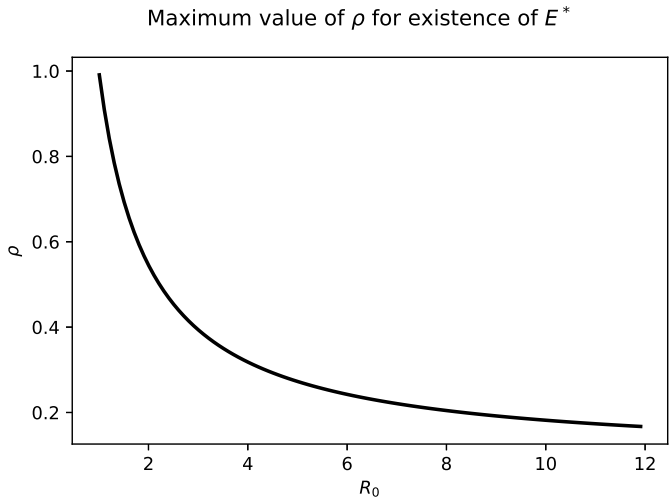

Figure 2. The maximum value of ρ allowing the existence of a biologically relevant chronic steady state in the system (14)–(16) as a function of R_0 values. It is seen that as R_0 becomes larger, infected hepatocyte proliferation must be increasingly impaired if a chronic infection state with a nonzero number of healthy hepatocytes is to exist. Note that in this example, the healthy hepatocyte proliferation rate is fixed at $r = 1$.

In contrast to the model studies by Hews et al. [36] in which infected hepatocytes could not divide, the fraction of infected hepatocytes at the chronic steady state in the model (14)–(16) now depends on the maximum proliferation rate of hepatocytes, even when that rate is small. In particular, that fraction is:

$$\frac{y^*}{x^*+y^*} = \frac{R_0-1}{\left(1-\frac{\rho}{r}\right)R_0}. \tag{17}$$

Notice that:

$$\lim_{\rho\to 0}\frac{y^*}{x^*+y^*} = \lim_{\rho\to 0}\frac{R_0-1}{\left(1-\frac{\rho}{r}\right)R_0} = 1-\frac{1}{R_0},$$

which is identical to the fraction of infected hepatocytes in the model without proliferating infected cells [36]. Figure 3 shows the percentage of infected hepatocytes for values of ρ

that yield a chronic state. Increasing ρ increases the fraction of infected hepatocytes. When $\rho = \frac{r}{R_0}$, E^* collides with E_i. For values of $\rho > \frac{r}{R_0}$, E^* is no longer biologically relevant.

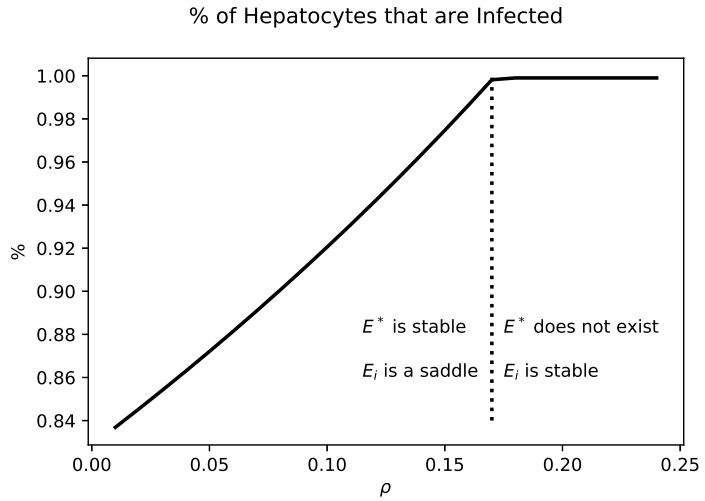

Figure 3. The fraction of infected hepatocytes at equilibrium, as a function of ρ, the infected hepatocyte proliferation rate. As this rate increases, more and more hepatocytes are infected, until a threshold is passed and the liver experiences 100% infection. When this point is crossed, there is also a stability switch as E_i^* shifts from stable to unstable, while E_i becomes stable. Other parameter values are fixed at $r = 1$, $K = 2 \times 10^{11}$, $\beta = 0.0014$, $\gamma = 200$, $a = 0.0693$, $\mu = 0.693$.

In drawing the connections between (7)–(9) and (14)–(16), we start by discussing the dynamics if the proliferation rate of infected hepatocytes is not severely impaired. This implies that $\rho > a$ and $\rho > \frac{r}{R_0}$. Therefore, E_i exists and E^* does not.

Proposition 3. *If $\rho > a$ and $\rho > \frac{r}{R_0}$, then E_f is unstable and E_i is locally asymptotically stable.*

Proof. The Jacobian matrix of the vector field corresponding to (14)–(16) at E_f is:

$$J(x,y,v)|_{E_f} = \begin{pmatrix} -r & -r & -\beta \\ 0 & -a & \beta \\ 0 & \gamma & -\mu \end{pmatrix}.$$

The eigenvalues of the matrix are given by:

$$\lambda_1 = -r, \tag{18}$$

$$\lambda_{2,3} = -\frac{1}{2}(a+\mu) \pm \frac{1}{2}\sqrt{(a+\mu)^2 - 4a\mu(1-R_0)}. \tag{19}$$

Since:

$$R_0 > \frac{r}{\rho} > 1,$$

$\lambda_{2,3}$ are positive and E_f is unstable.

The Jacobian matrix of the vector field corresponding to (14)–(16) at E_i is:

$$J(x,y,v)|_{E_i} = \begin{pmatrix} a\left(\frac{r}{\rho} - R_0\right) & 0 & 0 \\ -\rho + a + aR_0 & a-\rho & 0 \\ 0 & \gamma & -\mu \end{pmatrix}.$$

The eigenvalues are the following,

$$\begin{aligned}\lambda_1 &= -\mu,\\ \lambda_2 &= -(\rho - a),\\ \lambda_3 &= -a\left(R_0 - \frac{r}{\rho}\right).\end{aligned}$$

If $\rho > a$ and $R_0 > \frac{r}{\rho}$, then $\lambda_{1,2,3} < 0$ and E_i is locally asymptotically stable. □

According to Proposition 3, this model presents the following biological hypothesis: even if healthy and infected hepatocytes do not proliferate at the same rate, if the infected hepatocytes proliferate at a sufficiently high rate ($\rho > a$ and $\rho > \frac{1}{R_0}r$), then there will not be a significant population of healthy cells in the liver during chronic infection. Furthermore, with a sufficiently high infected hepatocyte proliferation rate, patients would be unlikely to experience oscillations in viral load and liver mass.

Impairing the maximum infected hepatocyte proliferation slightly impacts the following conditions: $\rho > a$ and $\rho > \frac{1}{R_0}r$. Although the chronic state E^* and the infected state E_i are both present, E_i is always unstable and the dynamics for (14)–(16) are similar to the model analyzed in Hews et al. [36].

Proposition 4. *For (14)–(16), if $\rho < \frac{1}{R_0}r$, then the following results hold.*
a. If $R_0 < 1$, then E_f is locally asymptotically stable and E_i is a saddle;
b. If $R_0 > 1$ then E_f is unstable and E_i is a saddle.

Since E_i exists, the global stability of E_f cannot be determined. As in Hews et al. [36], the severity of disease is controlled by R_0 and R^*. The bifurcation diagram (Figure 4) shows that for realistic R_0 values, there will be stable oscillations before passing through the Hopf bifurcation to experience liver failure.

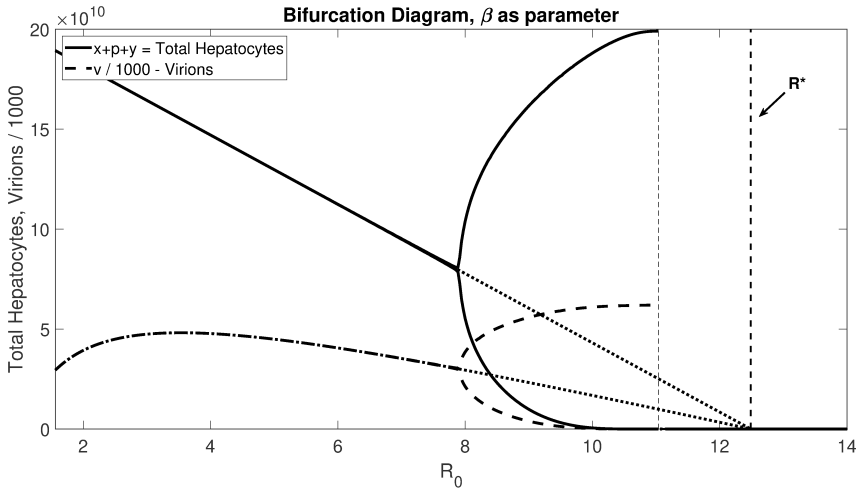

Figure 4. Bifurcation diagram showing equilibrium total hepatocyte and virion populations and oscillation bounds as a function of R_0, for the model with $r = \rho$, and R_0 controlled by changes in β. For R_0 below about 8, the total hepatocyte population falls nearly linearly with R_0, while sustained oscillations are observed for the approximate interval $R_0 \in (8, 11)$. A nonzero equilibrium still exists for R_0 up to the point that $R_0 = R^*$, where R^* is the cellular vitality index; beyond this, the system goes to the E_0 extinction equilibrium. The parameter values are $r = 0.8$, $\mu = 0.693$, $\gamma = 300$, and $K = 2 \times 10^{11}$.

We prove the existence of the Hopf bifurcation point below. Due to the extensive computations, we assumed that $\rho = 0$. Figure 4 suggests that this proof is valid for small ρ as well. As the reproductive number crosses the bifurcation point of $R_0 = 1$, the stability of

E_f is transferred to E^* as it crosses into the positive quadrant. Recall that E^* only exists in the positive quadrant when $1 \leq R_0 \leq R^*$. For the condition $R_0 \leq R^*$ to hold, the proliferation rate has to be sufficiently large; specifically, $r \geq \frac{\beta k - a\mu}{\mu}$.

Theorem 5. *Let* $\phi = a^2\left(\frac{R^*}{R_0} - 1\right)(R_0 - 1) + \frac{a^2}{R_0^2}(R_0 - 1) - \frac{ar}{R_0}(R_0 - 1) + a\mu\left(\frac{R^*}{R_0} - 1\right)$, *and* $\sigma = \frac{-(\mu a^2 R_0 + a^3 R^*)(R^* - R_0)(R_0 - 1)}{R_0(\mu R_0 + aR^*)}$. *If* $\phi > \sigma$, *then* E^* *is locally asymptotically stable.*

Proof.

$$J(x,y,v)|_{E_f} = \begin{pmatrix} r(1 - \frac{2x^*+y^*}{K}) - \frac{\beta v^* y^*}{(x^*+y^*)^2} & -\frac{rx^*}{K} + \frac{\beta v^* x^*}{(x^*+y^*)^2} & -\frac{\beta x^*}{x^*+y^*} \\ \frac{\beta v^* y^*}{(x^*+y^*)^2} & -\frac{\beta v^* x^*}{(x^*+y^*)^2} - a & \frac{\beta x^*}{x^*+y^*} \\ 0 & \gamma & -\mu \end{pmatrix}.$$

The eigenvalues of J satisfy:

$$\lambda^3 + a_2\lambda^2 + a_1\lambda + a_0 = 0,$$

where:

$$\begin{aligned} a_2 &= \mu + a\frac{R^*}{R_0}, \\ a_1 &= 2a^2\left(\frac{R^*}{R_0} - 1\right)(R_0 - 1) + \frac{a^2}{R_0^2}(R_0 - 1)^2 - \frac{ar}{R_0}(R_0 - 1) + a\mu\left(\frac{R^*}{R_0} - 1\right), \\ a_0 &= a^2\mu(R_0 - 1)\left(\frac{R^*}{R_0} - 1\right). \end{aligned}$$

Clearly, $a_2 > 0$ and $a_0 > 0$ when E^* exists. Let:

$$\phi = a^2\left(\frac{R^*}{R_0} - 1\right)(R_0 - 1) + \frac{a^2}{R_0^2}(R_0 - 1) - \frac{ar}{R_0}(R_0 - 1) + a\mu\left(\frac{R^*}{R_0} - 1\right),$$

where,

$$\begin{aligned} a_2a_1 - a_0 &= \mu a_2 + a\frac{R^*}{R_0}a_2 - a^2\mu(R_0 - 1)\left(\frac{R^*}{R_0} - 1\right), \\ &= \mu\phi + a\frac{R^*}{R_0}\phi + \left(\mu a^2 + a^3\frac{R^*}{R_0}\right)\left(\frac{R^*}{R_0} - 1\right)(R_0 - 1) > 0. \end{aligned} \tag{20}$$

Therefore, $a_2a_1 > a_0$ when:

$$\phi > \frac{-(\mu a^2 R_0 + a^3 R^*)(R^* - R_0)(R_0 - 1)}{R_0(\mu R_0 + aR^*)} = \sigma.$$

By the Routh–Hurwitz criteria, we determined a condition for E^* to be locally asymptotically stable. □

Theorem 6. *If* $a < a(R_0 - 1) < r$, *then there is a Hopf bifurcation at* $\phi = \sigma$.

Proof. Let $\Delta = a_2a_1 - a_0$. Then:

$$\Delta = \mu\phi + a\frac{R^*}{R_0}\phi + \left(\mu a^2 + a^3\frac{R^*}{R_0}\right)\left(\frac{R^*}{R_0} - 1\right)(R_0 - 1).$$

We showed above that $a_2a_1 = a_0$ when $\phi = \sigma$. Therefore, there exists an $r = r^*$ such that $\Delta(r^*) = 0$. Taking the partial derivative of Δ with respect to r, we obtain:

$$\begin{aligned}\frac{\partial \Delta}{\partial r} &= \mu\frac{\partial \phi}{\partial r} + \frac{aR^*}{R_0}\frac{\partial \phi}{\partial r} + \frac{\phi}{R_0} + \frac{\mu a}{R_0}(R_0-1) + \frac{a^2R^*}{R_0^2}(R_0-1) + \frac{a^2}{R_0}(R_0-1)\left(\frac{R^*}{R_0}-1\right),\\ &= 2\frac{\mu a}{R_0}(R_0-1) + \frac{\mu^2}{R_0} + 2\frac{a^2R^*}{R_0^2}(R_0-1) + \frac{a\mu R^*}{R_0^2} + \frac{\phi}{R_0}\\ &\quad + \frac{a^2}{R_0}(R_0-1)\left(\frac{R^*}{R_0}-1\right). \end{aligned} \tag{21}$$

When $\Delta = 0$, from (20), we obtain:

$$\frac{\phi}{R_0} = -\frac{\mu a^2}{\mu R_0 + aR^*}\left(\frac{R^*}{R_0}-1\right)(R_0-1) - \frac{a^3}{\mu R_0 + aR^*}\frac{R^*}{R_0}\left(\frac{R^*}{R_0}-1\right)(R_0-1). \tag{22}$$

Plugging (22) into (21) yields,

$$\begin{aligned}\frac{\partial \Delta}{\partial r}|_{\Delta=0} &= 2\frac{\mu a}{R_0}(R_0-1) + \frac{\mu^2}{R_0} + 2\frac{a^2R^*}{R_0^2}(R_0-1) + \frac{a\mu R^*}{R_0^2}\\ &\quad - \frac{\mu a^2}{\mu R_0 + aR^*}\left(\frac{R^*}{R_0}-1\right)(R_0-1) - \frac{a^3}{\mu R_0 + aR^*}\frac{R^*}{R_0}\left(\frac{R^*}{R_0}-1\right)(R_0-1)\\ &\quad + \frac{a^2}{R_0}(R_0-1)\left(\frac{R^*}{R_0}-1\right). \end{aligned} \tag{23}$$

Notice that,

$$\begin{aligned}\left[\frac{a^2R^*}{R_0^2} - \frac{a^2\mu}{\mu R_0 + aR^*}\left(\frac{R^*}{R_0}-1\right)\right](R_0-1) &= a\mu(R_0-1)\frac{a^2R^{*2} + a\mu R_0^2}{\mu R_0^2(\mu R_0 + aR^*)},\\ \left[-\frac{a^3}{\mu R_0 + aR^*}\frac{R^*}{R_0} + \frac{a^2}{R_0}\right](R_0-1)\left(\frac{R^*}{R_0}-1\right) &= \frac{a^2}{R_0}(R_0-1)\left(\frac{R^*}{R_0}-1\right)\left(\frac{\mu R_0}{\mu R_0 + aR^*}\right).\end{aligned}$$

Therefore,

$$\begin{aligned}\frac{\partial \Delta}{\partial r}|_{\Delta=0} &= 2\frac{\mu a}{R_0}(R_0-1) + \frac{\mu^2}{R_0} + \frac{a^2R^*}{R_0^2}(R_0-1) + \frac{a\mu R^*}{R_0^2} + a\mu(R_0-1)\frac{a^2R^{*2} + a\mu R_0^2}{\mu R_0^2(\mu R_0 + aR^*)}\\ &\quad + \frac{a^2}{R_0}(R_0-1)\left(\frac{R^*}{R_0}-1\right)\left(\frac{\mu R_0}{\mu R_0 + aR^*}\right) > 0.\end{aligned}$$

The two criteria (CH.1) and (CH.2) from Beretta and Kuang [45] are satisfied. Therefore, there is a Hopf bifurcation at $\phi = \sigma$. □

According to Proposition 4(b), Theorems 5 and 6, this model presents the following biological hypothesis: if the infected hepatocytes proliferation rate is significantly compromised, then there will be a significant population of healthy cells in the liver during chronic infection and patients would be likely to experience oscillations in viral load and liver mass.

Further impairing the maximum proliferation rate of infected hepatocytes implies that $\rho < a$ and $\rho < \frac{r}{R_0}$. Notice that further reducing ρ causes convergence to the model discussed in Hews et al. [36]. Since the existence of the Hopf bifurcation point is proven above, we will only evaluate the global stability result of E_f.

Proposition 7. *If $\rho < a$ and $R_0 < 1$, then E_f is globally stable.*

The proof for Proposition 7 is similar to that of Theorem 2, so we omit it here. These results show that dynamically, there is no benefit to including ρ in the model. If the rate of

proliferating infected hepatocytes is not significantly compromised, then one can safely assume that $\rho = r$; otherwise, one can safely assume that $\rho = 0$.

3. Global Stability Result for E_0

For a sufficiently virulent infection and small proliferation rate of the infected hepatocytes, the liver will completely fail. Mathematically, this situation is represented by the global asymptotic stability of the liver failure state, E_0. This section builds towards proving that if $R_0 > \left(\frac{r}{\mu}+1\right)R^*$ and $\rho < a < \mu + \rho$, then E_0 is globally stable. This technique is modified from Hews et al. [36]. The "blow-up transformation" has been used previously to study similar complex equilibrium [46–48]. Notice that a similar argument can be used for (7)–(9) to prove that if $R_0 > \frac{r+\mu}{\mu}$ and $r < a < \mu + r$, then E_0 is globally stable.

Since there is a singularity at the liver failure state, E_0, we used a ratio dependent transformation to arrive at the global result. We used the transformation $(x, y, v) \to (x, z, w)$, where $z = \frac{y}{x}$ and $w = \frac{v}{x}$. This results in the following system,

$$\frac{dx}{dt} = rx(t)\left(1 - \frac{x(t)+y(t)}{K}\right) - \frac{\beta w(t)x(t)}{1+z(t)}, \tag{24}$$

$$\frac{dz}{dt} = (\rho - r)z(t)\left(1 - \frac{x(t)+y(t)}{K}\right) + \beta w(t) - az(t), \tag{25}$$

$$\frac{dw}{dt} = \gamma z(t) - \mu w(t) - rw(t)\left(1 - \frac{x(t)(1+z(t))}{K}\right) + \frac{\beta w(t)^2}{1+z(t)}. \tag{26}$$

The steady states of (24)–(26) are:

$$U_0 = (0,0,0), \qquad U_n = (0, z_n, w_n), \qquad U_f = (K,0,0), \qquad U^* = (x^*, z^*, w^*),$$

where:

$$z_n = \frac{R^*(1+\frac{r}{\mu}) - R_0}{R^*(\frac{a}{\mu} - \frac{\rho}{\mu} - 1) + R_0}, \qquad w_n = \frac{aR^*}{\beta}z_n, \tag{27}$$

and:

$$x^* = \frac{Kra}{(r-\rho)^2}(1 - \frac{\rho}{r}R_0)\left(\frac{R^*}{R_0} - 1\right), \qquad z^* = \frac{R_0 - 1}{1 - \frac{\rho}{r}R_0}, \qquad w^* = \frac{\gamma(R_0-1)}{\mu(1-\frac{\rho}{r}R_0)}. \tag{28}$$

Notice that U_n is nonnegative when $\frac{\rho}{\mu} - \frac{a}{\mu} < \frac{R_0}{R^*} - 1 < \frac{r}{\mu}$ and U^* is nonnegative when $R^* < R_0 < 1$ and $R_0 < \frac{r}{\rho}$. The nontrivial steady states are preserved in that $E_f = U_f$ and $E^* = U^*$. E_0 has been blown up into two steady states: U_0 and U_n. We call these the two trivial states. To find a global stability result for E_0, we show that if $R_0 > \left(\frac{r}{\mu}+1\right)R^*$ and $\rho < a < \mu + \rho$, all steady states of (24)–(26) are unstable and that $\liminf_{t\to\infty} x = 0$ and $\limsup_{t\to\infty} z, w = \infty$. Since $y = xz$, $v = xw$, and (14)–(16) is bounded, this is enough to show if $R_0 > \left(\frac{r}{\mu}+1\right)R^*$ and $\rho < a < \mu + \rho$, then $\liminf_{t\to\infty} x, y, v = 0$.

Lemma 8. *U_0 and U_n are always unstable.*

Proof. The variational matrix of the system (24)–(26) evaluated at U_0 is:

$$J(x,z,w)|_{E_0} = \begin{pmatrix} r & 0 & 0 \\ -r & -aR^* & \beta \\ 0 & \gamma & -(\mu+r) \end{pmatrix}.$$

Since $\lambda_1 = r > 0$, U_0 is always unstable.

The variational matrix of the system (24)–(26) evaluated at U_n is:

$$J(x,z,w)|_{U_n} = \begin{pmatrix} r-\beta\frac{w_n}{1+z_n} & 0 & 0 \\ \frac{r-\rho}{K}z_n(1+z_n) & -aR^* & \beta \\ \frac{r}{K}w_n(1+z_n) & \gamma-\beta\frac{w_n^2}{(1+z_n)^2} & -\mu-r+2\beta\frac{w_n}{1+z_n} \end{pmatrix}.$$

$\lambda_1 = r-\beta\frac{w_n}{1+z_n} = \mu\left(\frac{R_0}{R^*}-1\right)$, which is negative when $R_0 < R^*$. On the other hand, $\lambda_{2,3}$ are given by the following matrix,

$$A = \begin{pmatrix} -aR^* & \beta \\ \gamma-\frac{\beta w_n^2}{(1+z_n)^2} & -\mu-r+2\beta\frac{w_n}{1+z_n} \end{pmatrix},$$

where:

$$tr(A) = -a-2r-\mu-z_n(\mu-a).$$

The trace is negative when $-\frac{a+\mu}{2} < \lambda_1$. However,

$$\det(A) = a\mu\left[\frac{R_0}{1+z_n}-\frac{(\mu+r)R^*}{(1+z_n)\mu}\right],$$

which is positive when $R_0 > (1+\frac{r}{\mu})R^*$. This condition and the condition for $\lambda_1 < 0$ contradict, so U_n is always unstable. □

Lemma 9. *If* $R_0 > (\frac{r}{\mu}+1)R^*$, *then* $\limsup_{t\to\infty} z(t), w(t) = \infty$.

Proof. Let $(z(t), w(t))$ be a solution of:

$$\begin{aligned} \frac{dz}{dt} &= \beta w - az + (\rho-r)z\left(1-\frac{x(1+z)}{K}\right) \geq \beta w-(a+r-\rho)z, \\ \frac{dw}{dt} &= \gamma z-\mu w-rw\left(1-\frac{x(1+z)}{K}\right)+\frac{\beta w^2}{1+z} \geq \gamma z-(\mu+r)w. \end{aligned}$$

Let $(Z(t), W(t))$ be a solution of:

$$\frac{dZ}{dt} = \beta W-(a+r-\rho)Z, \tag{29}$$

$$\frac{dW}{dt} = \gamma Z-(\mu+r)W. \tag{30}$$

$(Z,W) = (0,0)$ is the only steady state of (29) and (30) and is unstable when $R_0 > (\frac{r}{\mu}+1)R^*$. Since there are no other steady states, Z, W are unbounded, and (29) and (30) is a cooperative, monotone system, that is $\lim_{t\to\infty} Z(t), W(t) = \infty$. Let $z_0 = Z_0$ and $w_0 = W_0$, then by the comparison theorem, $(z(t), w(t)) \geq (Z(t), W(t))$ for $t > 0$. Therefore,

$$\liminf_{t\to\infty} z(t) \geq \lim_{t\to\infty} Z(t) = \infty,$$

$$\liminf_{t\to\infty} w(t) \geq \lim_{t\to\infty} W(t) = \infty.$$

Therefore, $\liminf_{t\to\infty} z(t), w(t) = \infty$. □

Theorem 10. *If* $R_0 > (\frac{r}{\mu}+1)R^*$ *and* $\rho < a < \mu+\rho$, *then* $\lim_{t\to\infty} x(t) = 0$.

Proof. To prove that E_0 is globally stable, we need it to be the only steady state in $\mathcal{R}^+$. Therefore, set $\rho < a$ to ensure that E_i no longer exists. Since:

$$\frac{dx}{dt} = rx(t)\left(1 - \frac{x(t)(1+z(t))}{K}\right) - \frac{\beta w(t)x(t)}{1+z(t)} < \left(r - \frac{\beta w(t)}{1+z(t)}\right)x(t),$$

it is sufficient to show:

$$\liminf_{t\to\infty} \frac{\beta w(t)}{1+z(t)} > r. \tag{31}$$

Let $\theta(t) = \frac{\beta w(t)}{1+z(t)}$. Then:

$$\begin{aligned}\frac{d\theta}{dt} &= \frac{\beta\frac{dw}{dt}}{1+z(t)} - \frac{\beta w(t)\frac{dz}{dt}}{(1+z(t))^2} \\ &= [\beta k + (a+r-\rho)\theta(t)]\frac{z(t)}{1+z(t)} - (\mu+r)\theta(t) \qquad (32)\\ &\quad + \frac{\beta w(t)x(t)}{K}\left(r + (\rho-r)\frac{z(t)}{1+z(t)}\right). \qquad (33)\end{aligned}$$

By Lemma (9), for all $\epsilon > 0$, $\exists\, t^*$ s.t. $\forall\, t \geq t^*$,

$$\frac{z(t)}{1+z(t)} > 1 - \epsilon. \tag{34}$$

Combining (32) and (34) for $t \geq t^*$,

$$\begin{aligned}\frac{d\theta}{dt} &> \beta k(1-\epsilon) + ((a+r-\rho)(1-\epsilon) - \mu - r)\theta(t) + \frac{\beta w(t)x(t)}{K}(\rho(1-\epsilon) + r\epsilon) \\ &> \beta k(1-\epsilon) + ((a+r-\rho)(1-\epsilon) - \mu - r)\theta(t).\end{aligned}$$

Letting $\Gamma(\epsilon) = (a+r-\rho)(1-\epsilon) - \mu - r$ and solving for $\theta(t)$ yields:

$$\theta(t) > \frac{\beta k(1-\epsilon)}{-\Gamma(\epsilon)} + \theta(t^*)e^{\Gamma(\epsilon)(t-t^*)} = \Theta(t).$$

Since $\rho < a < \mu + \rho$, $\Gamma(\epsilon) < 0$. Therefore, $\lim_{t\to\infty} \Theta(t) = \frac{\beta k(1-\epsilon)}{-\Gamma(\epsilon)}$. Since $R_0 > (\frac{r}{\mu} + 1)R^*$, $\exists\, \epsilon^* > 0$ s.t. $\forall\ \epsilon \in (0, \epsilon^*]$, $\frac{\beta k(1-\epsilon)}{\mu+r} > a + r$. Therefore,

$$\liminf_{t\to\infty} \frac{\beta w(t)}{1+z(t)} \geq \frac{\beta k(1-\epsilon)}{-\Gamma(\epsilon)} > \frac{\beta k(1-\epsilon)}{\mu+r} > a + r > r.$$

Thus, (31) is satisfied. □

According to Lemma 8, Lemma 9, and Theorem 10, this model presents the following biological hypothesis: if there is a sufficiently virulent infection and a small proliferation rate of infected hepatocytes, then the liver will fail.

Note that Theorem 3.3 only provides sufficient conditions for the collapse of the hepatocyte population, which can happen before R_0 is larger than $\left(1 + \frac{r}{\mu}\right)R^*$, as shown in Figure 4. This leaves an open mathematical question for a necessary condition for the collapse of the hepatocyte population.

4. Discussion

The effectiveness of treatment may be measured by its effect on R_0. Any reduction in R_0 that fails to cross $R_0 = 1$ from the right will not clear the infection and is a failure in this sense. However, it may still improve symptoms and reduce the likelihood of liver failure. If treatment reduces $R_0 < 1$, then it is curative if this reduction can be maintained under

the assumptions of the model. In the case of HBV, treatment with nucleoside analogues usually eventually fails. Mathematically, R_0 wanders under treatment, and while it may fall to less than one transiently, it eventually transits unity from the left. However, as a practical matter, R_0 need not be calculated to identify treatment failure.

The emergence of the cellular vitality index suggests a new way to classify the dynamics and plan the treatment of chronic HBV. Traditional therapies that target the virus affect only R_0, but R^* also determines when the liver fails. Given the limitation of the current standard of care, new treatment options are needed. Our model suggests that increasing healthy hepatocyte proliferation, decreasing infected hepatocyte proliferation, and increasing healthy and infected hepatocytes by the same factor should delay liver failure and promote patient survival. Since patients become resistant to all nucleoside analogues over time, further treatment options are needed. Our model proposes that controlling the proliferation rate should prolong the life of the liver. Increasing the distance between the cell vitality index and the reproduction number moves the Hopf bifurcation and decreases the likelihood of the onset of dangerous oscillations in liver damage. Specifically, the closer R_0 to R^*, the more likely the system will experience an oscillation or a collapse; see Figure 4. Thus, increasing the distance, for example by controlling the proliferation rate, can prevent this dangerous onset. Treatment options that control the proliferation rate of healthy and infected hepatocytes are not currently available and, to the best of our knowledge, are not currently being explored.

These model conclusions only hold if proliferation in infected cells leads to infected daughter cells. However, experimental evidence suggests that hepatocyte proliferation may destabilize and dilute viral DNA, thus aiding in clearing infection [49], and that hepatocyte proliferation may be inversely associated with viral loads in experimental settings. Furthermore, modeling work by Goyal et al. [42] suggests hepatocyte division may be an important mechanism in both clearing infection and protecting the liver from catastrophic cell loss. It is unclear, however, the degree to which these possible protective properties of proliferation are at work in acute vs. chronic infection.

The model analysis suggests that the modeling decision to include proliferating infected hepatocytes in an HBV model should depend on whether or not the proliferation rate of infected hepatocytes is severely impaired. If it is not, then including a slightly different proliferation rate of infected hepatocytes compared to uninfected cells adds needless complexity; the key dynamics will be essentially unaltered, so it is safe to assume that infected and uninfected cells proliferate at the same rate. On the other hand, if infection significantly impairs the proliferative potential of hepatocytes, then one can safely assume that infected cells do not proliferate; again, the dynamical behavior is insensitive to variations in the rate at which infected cells divide.

The analysis presented here also suggests a testable biological prediction, namely that one can determine if infected hepatocytes are proliferating to an appreciable degree, and yielding infected daughter cells, simply by searching for uninfected cells. If all cells in the liver are infected (beyond the acute phase of infection), then this model proposes that infected cells are proliferating at a high rate and generating infected progeny. The existence of a significant uninfected population implies the severely impaired proliferative potential of infected cells. It has been observed that the fraction of hepatocytes infected in a chronic HBV case progresses from nearly to 100% to only a few percent [50]. This may be explained by a combination of gradual immune attrition of infected hepatocytes, possibly impaired viral replication, and weak proliferation. Mason et al. [50] recently presented evidence that hepatocytes refractory to infection are selected over the course of chronic infection, with healthy clonal populations prevalent. Thus, it is likely that a strong proliferative advantage for healthy over infected cells can keep infected hepatocyte populations low through both Darwinian mechanisms and via the intrinsic population dynamics of the disease system.

Our minimal representation of the immune response is also a clear limitation, but by minimizing model dimensionality, we can more clearly elucidate the effect of comparative proliferation rates on the model dynamics. An essential component of the immune response,

at least in acute HBV infection, may be noncytotoxic curing of infected cells with subsequent "immunity" to re-infection, considered in modeling works by Ciupe et al. [16,37]. This dynamic cannot be considered in our current framework and may have further implications for the role of proliferation among different hepatocyte populations.

Future work will also focus on using the model to explore the impact of treatments. Current antiviral therapies include standard interferon and PEGylated interferon therapies for short-term use and nucleoside/nucleotide analogues for long-term use [51–53], but there are still open questions about the optimum timing and ordering of the treatments [54,55]. Models that have made slightly different assumptions have fit their models to existing datasets showing complex virus dynamics resulting from clinical trials [22,27,29,37,38,41,43,56–58].

One should take care, however, not to push this model, and therefore the hypothesis just presented, too far. The BVIM has typically been applied to infections of the blood (e.g., malaria and HIV). However, unlike blood, the tissues of the liver are not well mixed, which raises legitimate questions about the validity of an ODE description. Therefore, an important future project is to study a spatially explicit version of this model. The most obvious approach would be a partial differential equation model in which the basic dynamical properties modeled here are coupled with terms describing virion diffusion through the interstitium and perhaps a form of advection representing the passage of virions through the hepatic vasculature. At any rate, the significance of spatial effects is an open question that needs to be addressed before long.

Author Contributions: Conceptualization, S.H., S.E., J.D.N. and Y.K.; investigation, S.H., S.E., J.D.N., T.P. and Y.K.; writing—original draft preparation, S.H., S.E., J.D.N. and Y.K.; writing—review and editing, S.H., S.E., J.D.N., T.P. and Y.K.; visualization, S.H., S.E. and Y.K.; supervision, J.D.N. and Y.K.; project administration, Y.K.; funding acquisition, Y.K. All authors read and agree to the published version of the manuscript.

Funding: Research of Yang Kuang is partially supported by NSF Grant DEB-1930728 and NIH Grant 5R01GM131405-02.

Acknowledgments: The authors would like to thank the reviewers for their many helpful comments and suggestions.

Conflicts of Interest: The authors declare no conflict of interest.

References

1. Arguin, P.; Kozarsky, P.; Reed, C. (Eds.) *CDC Health Information for International Travel 2008*; Elsevier: Philadelphia, PA, USA, 2007.
2. World Health Organization. *Heptatitis B Fact Sheet*; World Health Organization: Geneva, Switzerland, 2020.
3. Locarnini, S.; Hatzakis, A.; Chen, D.; Lok, A. Strategies to control hepatitis B: Public policy, epidemiology, vaccine and drugs. *J. Hepatol.* **2015**, *62*, S76–S86. [CrossRef]
4. Chen, Y.; Tian, Z. HBV-Induced Immune Imbalance in the Development of HCC. *Front. Immunol.* **2019**, *10*, 2048. [CrossRef]
5. Guidotti, L.; Chisari, F. Immunobiology and Pathogenesis of Viral Hepatitis. *Annu. Rev. Pathol. Mech. Dis.* **2006**, *1*, 23–61. [CrossRef]
6. Rehermann, B. Pathogenesis of Chronic Viral Hepatitis: Differential Roles of T Cells and NK Cells. *Nat. Med.* **2013**, *19*, 859–868. [CrossRef]
7. Pang, X.; Li, X.; Mo, Z.; Huang, J.; Deng, H.; Lei, Z.; Zheng, X.; Feng, Z.; Xie, D.; Gao, Z. IFI16 is Involved in HBV-Associated Acute-on-Chronic LIver Failure Inflammation. *BMC Gastroenterol.* **2018**, *18*, 61. [CrossRef]
8. Seeger, C.; Mason, W.S. Molecular Biology of Hepatitis B Virus Infection. *Virology* **2015**, *479-480*, 672–686. [CrossRef] [PubMed]
9. Zhang, Y.Y.; Hu, K.Q. Rethinking the Pathogenesis of Hepatitis B Virus (HBV) Infection. *J. Med. Virol.* **2015**, *87*, 1989–1999. [CrossRef] [PubMed]
10. Kwun, H.; Jang, K. Natural variants of hepatitis B virus X protein have differential effects on the expression of cyclin-dependent kinase inhibitor p21 gene. *Nucleic Acids Res.* **2004**, *32*, 2202–2213. [CrossRef]
11. Wu, B.; Li, C.; Chen, H.; Chang, J.; Jeng, K.; Chou, C.; Hsu, M.; Tsai, T. Blocking of G1/S transition and cell death in the regenerating liver of hepatitis B virus X protein transgenic mice. *Biochem. Biophys. Res. Commun.* **2006**, *340*, 916–928. [CrossRef] [PubMed]
12. Dong, Z.; Zhang, J.; Sun, R.; Wei, H.; Tian, Z. Impairment of liver regeneration correlates with activated hepatic NKT cells in HBV transgenic mice. *Hepatology* **2007**, *45*, 1400–1412. [CrossRef]

13. Tralhao, J.G.; Roudier, J.; Morosan, S.; Giannini, C.; Tu, H.; Goulenok, C.; Carnot, F.; Zavala, F.; Joulin, V.; Kremsdorf, D.; et al. Paracrine in vivo inhibitory effects of hepatitis B virus X protein (HBx) on liver cell proliferation: An alternative mechanism of HBx-related pathogenesis. *Proc. Natl. Acad. Sci. USA* **2002**, *99*, 6991–6996. [CrossRef]
14. Hodgson, A.; Keasler, V.; Slagle, B. Premature cell cycle entry induced by hepatitis B virus regulatory HBx protein during compensatory liver regeneration. *Cancer Res.* **2008**, *68*, 10341–10348. [CrossRef]
15. Goyal, A.; Liao, L.; Perelson, A. Within-host mathematical models of hepatitis B virus infection: Past, present, and future. *Curr. Opin. Syst. Biol.* **2019**, *18*, 27–35. [CrossRef]
16. Ciupe, S. Modeling the dynamics of hepatitis B infection, immunity, and drug therapy. *Immunol. Rev.* **2018**, *285*, 38–54. [CrossRef]
17. Nowak, M.; Bonhoeffer, S.; Hill, A.; Boehme, R.; Thomas, H.; McDade, H. Viral dynamics in hepatitis B virus infection. *Proc. Natl. Acad. Sci. USA* **1996**, *93*, 4398–4402. [CrossRef] [PubMed]
18. Nowak, M.; May, R. *Virus Dynamics*; Oxford University Press: Oxford, UK, 2000.
19. Leenheer, P.D.; Smith, H. Virus dynamics: A global analysis. *SIAM J. Appl. Math.* **2003**, *63*, 1313–1327.
20. Perelson, A.; Nelson, P. Mathematical analysis of HIV-1 dynamics in vivo. *SIAM Rev.* **1999**, *41*, 3–44. [CrossRef]
21. Allali, K.; Meskaf, A.; Tridane, A. Mathematical modeling of the adaptive immune responses in the early stage of the HBV infection. *Int. J. Differ. Equ.* **2018**, *2018*, 6710575. [CrossRef]
22. Ciupe, S.; Ribeiro, R.M.; Nelson, P.; Dusheiko, G.; Perelson, A. The role of cells refractory to productive infection in acute hepatitis B viral dynamics. *Proc. Natl. Acad. Sci. USA* **2007**, *104*, 5050–5055. [CrossRef] [PubMed]
23. Wang, K.; Jin, Y.; Fan, A. The effect of immune responses in viral infections: A mathematical model view. *Discret. Contin. Dyn. Syst.-Ser. B* **2014**, *19*, 3379–3396. [CrossRef]
24. Yousfi, N.; Hattaf, K.; Tridane, A. Modeling the adaptive immune response in HBV infection. *J. Math. Biol.* **2011**, *63*, 933–957. [CrossRef]
25. Forde, J.; Ciupe, S.; Cintron-Arias, A.; Lenhart, S. Optimal control of drug therapy in a hepatitis B model. *Appl. Sci.* **2016**, *6*, 219. [CrossRef]
26. Tridane, A.; Hattaf, K.; Yafia, R.; Rihan, F. Mathematical modeling of HBV with the antiviral therapy for the immunocompromised patients. *Commun. Math. Biol. Neurosci.* **2016**, *2016*, 20.
27. Kim, H.; Kwon, H.; Jang, T.; Lim, J.; Lee, H. Mathematical modeling of triphasic viral dynamics in patients with HBeAg-positive chronic hepatitis B showing response to 24-week clevudine therapy. *PLoS ONE* **2012**, *7*, e50377. [CrossRef] [PubMed]
28. Ribeiro, R.; Lo, A.; Perelson, A. Dynamics of hepatitis B virus infection. *Microb. Infect.* **2002**, *4*, 829–835. [CrossRef]
29. Ribeiro, R.; Germanidis, G.; Powers, K.; Pellegrin, B.; Nikolaidis, P.; Perelson, A.; Pawlotsky, J. Hepatitis B virus kinetics under antiviral therapy sheds light on differences in hepatitis B e antigen positive and negative infections. *J. Infec. Dis.* **2010**, *202*, 1309–1318. [CrossRef]
30. Gourley, S.; Kuang, Y.; Nagy, J. Dynamics of a delay differential model of hepatitis B virus. *J. Biol. Dyn.* **2008**, *2*, 140–153. [CrossRef] [PubMed]
31. Min, L.; Su, Y.; Kuang, Y. Mathematical Analysis of a Basic Virus Infection Model with Application to HBV Infection. *Rocky Mt. J. Math.* **2008**, *38*, 1573–1585 . [CrossRef]
32. Hattaf, K.; Yousfi, N.; Tridane, A. Mathematical analysis of a virus dynamics model with general incidence rate and cure rate. *Nonlinear Anal. Real World Appl.* **2012**, *13*, 1866–1872. [CrossRef]
33. Hattaf, K.; Yousfi, N.; Tridane, A. Stability analysis of a virus dynamics model with general incidence rate and two delays. *Appl. Math. Comput.* **2013**, *221*, 514–521. [CrossRef]
34. Kuang, Y.; Nagy, J.; Eikenberry, S.E. *Introduction to Mathematical Oncology*; CRC Press: Boca Raton, FL, USA, 2018.
35. Eikenberry, S.; Hews, S.; Nagy, J.D.; Kuang, Y. The Dynamics of a Delay Model of HBV Infection with Logistic Hepatocyte Growth. *Math. Biosci. Eng.* **2008**, *6*, 283–299.
36. Hews, S.; Eikenberry, S.; Nagy, J.D.; Kuang, Y. Rich dynamics of a hepatitis B viral infection model with logistic hepatocyte growth. *J. Math. Biol.* **2009**, *60*, 573–590. [CrossRef]
37. Ciupe, S.; Ribeiro, R.; Nelson, P.; Perelson, A. Modeling the mechanisms of acute hepatitis B virus infection. *J. Theoret. Biol.* **2007**, *247*, 23–35. [CrossRef]
38. Dahari, H.; Shudo, E.; Ribeiro, R.M.; Perelson, A. Modeling complex decay profiles of hepatitis B virus during antiviral therapy. *Hepatology* **2009**, *49*, 32–38. [CrossRef] [PubMed]
39. Reluga, T.; Dahari, H.; Perelson, A. Analysis of hepatitis C virus infection models with hepatocyte homeostasis. *SIAM J. Appl. Math.* **2009**, *69*, 999–1023. [CrossRef] [PubMed]
40. Ciupe, S.; Hews, S. Mathematical models of e-antigen mediated immune tolerance and activation following prenatal HBV infection. *PLoS ONE* **2012**, *7*, e39591. [CrossRef] [PubMed]
41. Ciupe, S.; Ribeiro, R.; Perelson, A. Antibody responses during hepatitis B viral infection. *PLoS Comput. Biol.* **2014**, *10*, e1003730. [CrossRef]
42. Goyal, A.; Ribeiro, R.; Perelson, A. The role of infected cell proliferation in the clearance of acute HBV infection in humans HBV infection in humans. *Viruses* **2017**, *9*, 350. [CrossRef]
43. Rodriguez, A.; Chung, M.; Ciupe, S. Understanding the complex patterns observed during hepatitis B virus therapy. *Viruses* **2017**, *9*, 117. [CrossRef] [PubMed]

44. Ciupe, S.; Catllá, A.; Forde, J.; Schaeffer, D. Dynamics of hepatitis B virus infection: What causes viral clearance? *Math. Popul. Stud.* **2011**, *18*, 87–105. [CrossRef]
45. Beretta, E.; Kuang, Y. Modeling and analysis of a marine bacteriophage infection. *Math. Biosci.* **1998**, *149*, 57–76. [CrossRef]
46. Hsu, S.B.; Hwang, T.W.; Kuang, Y. Global analysis of the Michaelis–Menten-type ratio-dependent predator-prey system. *J. Math. Biol.* **2001**, *42*, 489–506. [CrossRef] [PubMed]
47. Berezovskaya, F.; Karev, G.; Song, B.; Castillo-Chavez, C. A simple epidemic model with surprising dynamics. *Math. Biosci. Eng.* **2005**, *2*, 133. [CrossRef]
48. Phan, T.; Pell, B.; Kendig, A.E.; Borer, E.T.; Kuang, Y. Rich dynamics of a simple delay host-pathogen model of cell-to-cell infection for plant virus. *Discret. Contin. Dyn. Syst.-B* **2021**, *26*, 515.
49. Allweiss, L.; Volz, T.; Giersch, K.; Kah, J.; Raffa, G.; Petersen, J.; Lohse, A.W.; Beninati, C.; Pollicino, T.; Urban, S.; et al. Proliferation of primary human hepatocytes and prevention of hepatitis B virus reinfection efficiently deplete nuclear cccDNA in vivo. *Gut* **2018**, *67*, 542–552. [CrossRef] [PubMed]
50. Mason, W.S.; Liu, C.; Aldrich, C.E.; Litwin, S.; Yeh, M.M. Clonal expansion of normal-appearing human hepatocytes during chronic hepatitis B virus infection. *J. Virol.* **2010**, *84*, 8308–8315. [CrossRef]
51. Konerman, M.; Lok, A. Interferon treatment for hepatitis B. *Clin. Liver Dis.* **2016**, *20*, 645–665. [CrossRef]
52. Lampertico, P.; Aghemo, A.; Vigano, M.; Colombo, M. HBV and HCV therapy. *Viruses* **2009**, 484–509. [CrossRef]
53. Nguyen, M.; Wong, G.; Gane, E.; Kao, J.H.; Dusheiko, G. Hepatitis B Virus: Advances in Prevention, Diagnosis, and Therapy. *Clin. Microbiol. Rev.* **2020**, *33*, e00046-19. [CrossRef]
54. Block, T.; Locarnini, S.; McMahon, B.; Rehermann, B.; Peters, M. Use of current and new endpoints in the evaluation of experimental hepatitis B therapeutics. *Clin. Infec. Dis.* **2017**, *64*, 1283–1288. [CrossRef]
55. Lok, A.; McMahon, B.; Brown, R.; Wong, J.; Ahmed, A.; Farah, W.; Almasri, J.; Alahdab, F.; Benkhadra, K.; Mouchli, M.; et al. Antiviral therapy for chronic hepatitis B viral infection in adults: A systematic review and meta-analysis. *Hepatology* **2016**, *63*, 284–306. [CrossRef] [PubMed]
56. Colombatto, P.; Civitano, L.; Bizzarri, R.; Oliveri, F.; Choudhury, S.; Gieschke, R.; Bonino, F.; Brunetto, M. A multiphase model of the dynamics of HBV infection in HBeAg-negative patients during PEGylated interferon-alpha2a, lamivudine and combination therapy. *Antivir. Ther.* **2006**, *11*, 197–212. [PubMed]
57. Lewin, S.; Ribeiro, R.; Walters, T.; Lau, G.; Bowden, S.; Locarnini, S.; Perelson, A. Analysis of hepatitis B viral load decline under potent therapy: complex decay profiles observed. *Hepatology* **2001**, *34*, 1012–1020. [CrossRef] [PubMed]
58. Tsiang, M.; Rooney, J.; Toole, J.; Gibbs, G. Biphasic clearance kinetics of hepatitis B virus from patients during adefovir dipivoxil therapy. *Hepatology* **1999**, *29*, 1863–1869. [CrossRef] [PubMed]